Hard Coatings on Ti-Based Materials Produced by Weld Deposition

Yahea Malek Hussien[a*], Vivek C. Peddiraju[a] S. Suryakumar[b], Bharat B. Panigrahi[a], and Subhradeep Chatterjee[a]

Indian Institute of Hyderabad, Sangareddy-502284, India,
[a]Department of Materials Science and Metallurgical Engineering and [b]Department of Mechanical and Aerospace Engineering, India
ms24mtech16001@iith.ac.in

Abstract. Weld deposition of nickel on titanium-based materials can be used effectively for surface alloying and hardening. Here we used an ER-Ni filler for depositing Ni on commercially pure Ti (CP-Ti) and Ti-6Al-4V (Ti-64) substrates. After melting and mixing with the substrate, Ti-Ni intermetallic compounds (IMCs) are formed in situ. We used optical and electron microscopy to characterize the fusion zone and reveal the presence of different IMCs. These were Ti_2Ni, NiTi, and Ni_3Ti for CP-Ti, and the same compounds were found to have dissolved Al and V for Ti-64. The spatial distribution of these phases was found to vary based on the location in the alloyed surface layer, with Ti_2Ni occurring mostly near the coating-substrate interface and top regions being a mixture of NiTi and Ni_3Ti. We measured the hardness of the coatings and correlated it with the local microstructure for each coating.

Keywords: Surface alloying of Titanium alloys; Weld deposition, Microhardness, Intermetallic Compounds

1 Introduction

Titanium alloys are used widely in aerospace, chemical, and biomedical applications due to their high specific strength and toughness, good corrosion resistance, and biocompatibility. However, they have poor tribological properties, especially wear resistance, which limits their application [1, 2]. These properties can be improved by surface modification, and the laser cladding technique has been widely employed for this purpose [3–5]. However, most of the cladding work involved either the addition of hard ceramic reinforcement phases, which get embedded in a metallic matrix, or the production of intermetallic compounds (IMCs) [6–10] during cladding to improve the hardness. For example, the generation of Ti-Al IMCs by using a Ti/Al-X (X: TiC, AlN, AlB2) powder system has been reported [11–13]. Ti-Ni IMC-based claddings have also been created on Ti using nickel-based powders [14, 15]. In addition, a few studies have used Ti with ceramic reinforcements in the powder system [7, 9, 16]. However, the use of an alternative technique of surface alloying using gas metal arc welding (GMAW),

S. Uppapalli and D. Chakraborty (eds.), *Proceedings of the International Conference on Mechanics, Materials and Mechatronics (ICM³ 2026)*, Atlantis Highlights in Engineering 47,
https://doi.org/10.2991/978-94-6239-764-4_10

which is a widely employed technique for hardfacing of steels, has been less explored for Ti-based materials. Here we report the use of a GMAW-based deposition method with pure nickel as a filler wire to produce surface-alloyed Ni-Ti layers on commercially pure titanium (CP-Ti) and Ti-6Al-4V (Ti-64) substrates. Similar to laser cladding, the metallurgical characteristics of the alloyed fusion zone produced by the melting and mixing of the filler and the substrate can be controlled by modifying the welding process parameters. The Ni-Ti system has three IMCs, viz. Ni_3Ti, NiTi, and Ti_2Ni, the first two of which melt congruently and the last by a peritectic reaction between the liquid and NiTi; these IMCs also form two eutectics, E1: Ti+Ti_2Ni and E2: NiTi+Ni_3Ti. Here, we report our findings in terms of the variation of composition, microstructure, and hardness as a function of the distance from the fusion interface in the substrate. Further analysis is performed to establish the origins of the formation of different IMCs and their correlation with the variation in hardness in the alloyed layer.

2 Material and methods

Pure nickel filler wire (ER-Ni) was deposited on commercially pure titanium and Ti-6Al-4V plates using the pulsed gas metal arc welding (GMAW-P) technique. A Fronius CMT Advanced 4000 R power source paired with an RCU 5000-i control is used for this welding. In this mode, the wire feed rate is controlled, and the current and voltage are dynamically adjusted by the control unit. To examine alloying and phase formation in the fusion zone, multi-track overlapping weld depositions were performed using the process parameters listed in Table 1. For microstructural characterization, we extracted samples from the coating region using an electro-discharge machine (EDM). Standard mounting, grading, polishing, and etching (4ml HF, 8ml H_2O_2, 90 ml H_2O) techniques were used to prepare metallographic samples. A Leica DM2700M optical microscope was employed to capture weld pool microstructures at low magnification. For observing features in more detail and ascertaining elemental mixing, a JEOL JIP-4700F scanning electron microscope (SEM) equipped with an energy-dispersive spectrometer (EDS) and a dedicated back-scattering electron (BSE) detector was used. Hardness variation in the samples was examined using a Vickers microindentation test (EMCO Durascan 20) with a load of 0.1 kgf for 10s.

Table 1: Welding parameters

Base material	**Insert atmosphere**	**Wire feed rate (m/min)**	**Current (A)**	**Voltage (V)**	**Travel speed (mm/min)**	**CTWD (mm)**	**Overlap**
CP-Ti	Ar	7	183	13.3	800	13	4
Ti-64	Ar	7	183	13.3	800	13	4.5

3 Results and discussion

Fig. 1 shows a collage of the longitudinal section macrostructure for both samples, CP-Ti and Ti-64, respectively. Here we can clearly notice the formation of three distinct regions in both samples: fusion zone, interface zone, and heat-affected zone. The fusion interface appears dark due to the over-etching required for revealing other features. The non-uniform contrast indicates the formation of different IMCs mixtures in Ni-Ti: differences in the etching rates of these phases, and hence in their topography, lead to the variation in contrast. Formation of a metallurgically bonded layer on top of the substrates was observed in both CP-Ti and Ti-64. The microstructures exhibit a fine cellular/dendritic structure near the top of the coating and slightly coarser features toward the bottom.

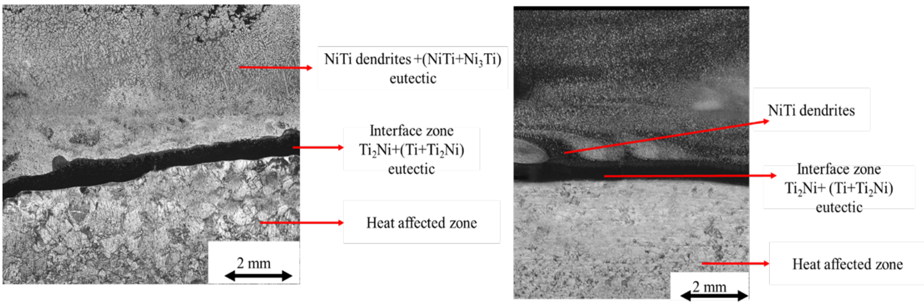

Fig. 1: Fusion zone macrostructure for (a) CP-Ti and (b) Ti-64

Variation in composition for both samples next to the fusion interface is presented in Fig. 2. It shows that as we transition from the base metal to the fusion zone, the nickel content rises steeply within a few hundred micrometers of the fusion interface and then fluctuates around a mean composition of 56 at. % Ni for CP-Ti and about 54 at.% Ni for Ti-64. For the latter, the Al and V contents also undergo sharp (but limited in extent) change near the fusion interface. Additional microstructural and compositional analyses indicate that the primary microstructural constituents of the fusion zone (FZ) are dendrites of Ti_2Ni, NiTi, and Ni_3Ti, together with eutectic structures of E1 and E2.

Fig. 3 shows the microstructural characteristics around the fusion interface and FZ of CP-Ti and Ti-64. Both materials showed similar characteristics at the fusion interface. In Fig. 3(a, c), we can observe columnar Ti_2Ni dendrites growing from the fusion zone side to the substrate. In addition, a eutectic structure (E1) having a composition of 27% at. Ni was identified, which corresponds to the eutectic reaction E1 ($L \rightarrow Ti+Ti_2Ni$) in the Ti-Ni phase diagram. For CP-Ti, a eutectic mixture of NiTi+Ni_3Ti was also found in the fusion zone (Fig. 3b) with a mean composition of about 65 at. % Ni. Similar to the CP-Ti sample, NiTi dendrites (with dissolved Al and V) were also found in the fusion zone of the Ti-64 sample, and a Ti_2Ni-based IMC could be identified between these dendritic

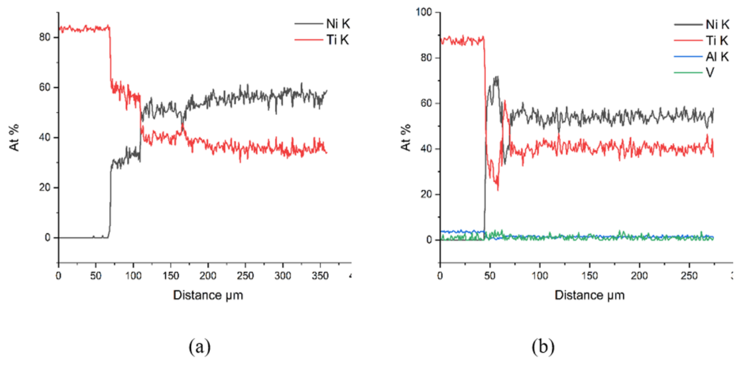

Fig. 2: Composition line-scans across the fusion zone for (a) CP-Ti and (b) Ti-64

regions, which formed via the peritectic interaction between the primary NiTi phase and the residual liquid after solidification (L+NiTi→Ti_2Ni) as per the Ti–Ni phase diagram.

Fig. 4 (a-b) shows the hardness variation for samples CP-Ti and Ti-64, respectively. In both cases, the hardness increases sharply from the substrate to a higher value in the fusion zone. The average hardness values in CP-Ti and Ti64 substrates are 500 HV and 700 HV, respectively. The hardness increased in both samples three times compared with the base metal using gas metal arc welding without adding any ceramic reinforcements. The higher hardness value corresponded to the regions having NiTi and E1 eutectic in CP-Ti and with NiTi and Ti_2Ni in Ti-64.

The microstructural variation across the fusion zone is shown schematically in Fig 4 (c-d). The observed heterogeneous microstructures can be explained on the basis of the Ti–Ni binary phase diagram and the compositional gradient formed during the deposition process. As the composition gradually changes from Ti-rich at the fusion interface to relatively Ni-rich at the top of the fusion zone, thermodynamically favorable conditions are created for the creation of various intermetallic phases. The fusion interface of both CP-Ti and Ti-64 specimens exhibited columnar Ti_2Ni dendrites and E1 eutectic structure Ti+Ti_2Ni.

With respect to the solidification direction, NiTi-rich regions were formed in the FZ towards the higher Ni-concentration areas (i.e., away from the fusion interface). In CP-Ti, an E2 eutectic structure of NiTi+Ni_3Ti was found in regions close to the top of the FZ, which showed local Ni enrichment under non-equilibrium solidification conditions. Ti-64, on the other hand, exhibited distinct solidification behavior where NiTi dendrites grew in the top FZ and Ti_2Ni phase grew between the dendrites.

We note that some cracks were observed in the fusion interface of Ti-64, whereas CP-Ti coating was free of cracks. While the brittle nature of the Ti_2Ni phase could have contributed to the observed cracking in the Ti-64 coating,

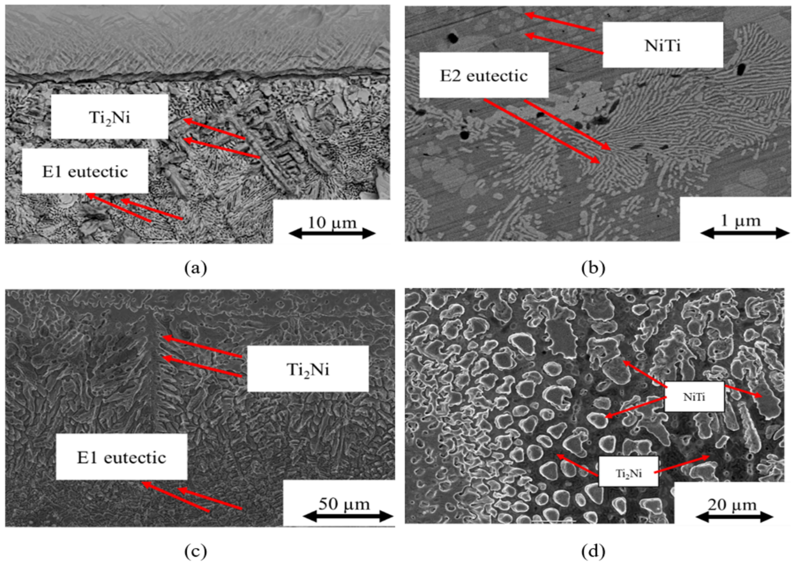

Fig. 3: (a) Fusion interface microstructure for CP-Ti, (b) Fusion zone microstructure for CP-Ti, (c) Fusion interface microstructure for Ti-64, (d) Fusion zone microstructure for Ti-64

absence of cracking or delamination in CP-Ti coating suggests other factors such as thermal stresses originating from the temperature are also likely involved.

The difference in the phases formed in the two cases can be understood in terms of the additional alloying elements Al and V which change the thermodynamics of the system, thereby changing the favorable growth conditions for different phases. The observed pattern may also be influenced by the overall composition of the fusion zone, particularly the relative amounts of Ni and Ti resulting from dilution, which can affect the solidification path and phase evolution during deposition. In all systems, complex heterogeneous microstructures containing dendritic intermetallic phases and eutectic constituents were significant in improving the hardness. The highest hardness values were observed in areas with NiTi dendrites and IMCs, owing to the composite strengthening effect. The enhanced hardness indicates the effectiveness of the surface alloying process in improving the surface characteristics of the coated specimens.

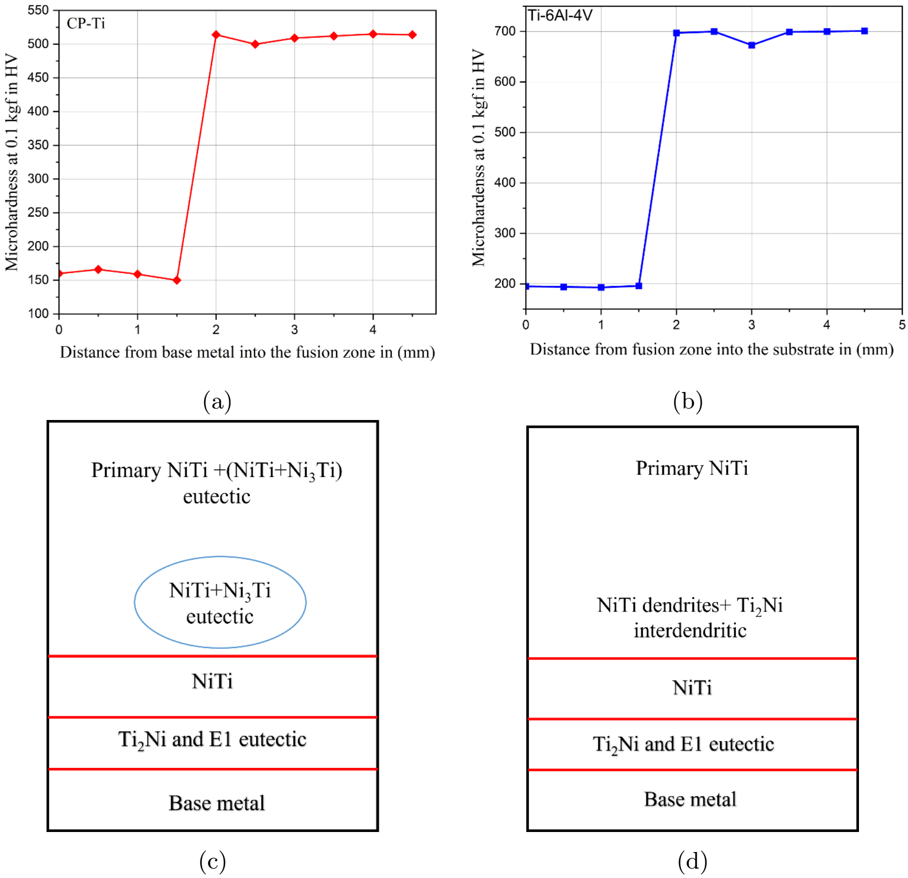

Fig. 4: Hardness variation from the base metal into the top surface in the fusion zone in (a) CP-Ti and (b) Ti-64. Schematic illustration of phase evolution and microstructure development in the FZ for (c) CP-Ti and (d) Ti-64.

To understand the underlying solidification mechanism and phase selection in the FZ, we carried out a thermodynamic simulation using Thermo-Calc® with TCNi9 and TCTi6 databases. These are aimed at determining the phases formed under thermodynamic equilibrium at a given temperature and their amounts when the substrate material (CP-Ti or Ti-64) is diluted by the addition of the filler Ni. The composition profiles in Fig. 2 show that the maximum Ni-content of the FZ is about 55 to 60 at.% for CP-Ti and Ti-64, respectively, the simulations are restricted within these limits. Fig. 5 compares the phase fractions for the two systems at 900 °C. The solidification of the FZ for CP-Ti is complete at this temperature and it consists of β-Ti, Ti_2Ni, NiTi and Ni_3Ti phases and corresponding two-phase mixtures as one moves progressively towards higher

Ni-content away from the fusion interface. In contrast, the simulation for Ti-64 shows that the Ni-rich part of the FZ is still liquid at this temperature, indicating the effect of Al and V addition on the liquidus surface. In addition, there are significant changes in the composition windows in which different phases appear with changes in their amounts as well. Importantly, the Ni_3Ti phase seems to have become restricted to a very narrow band of composition in Ti-64/Ni, which is in broad agreement with the experimental observations. Thus, the persistence of liquid and altered phase stability are expected to influence phase evolution during solidification and contribute to the experimentally observed differences in the microstructure.

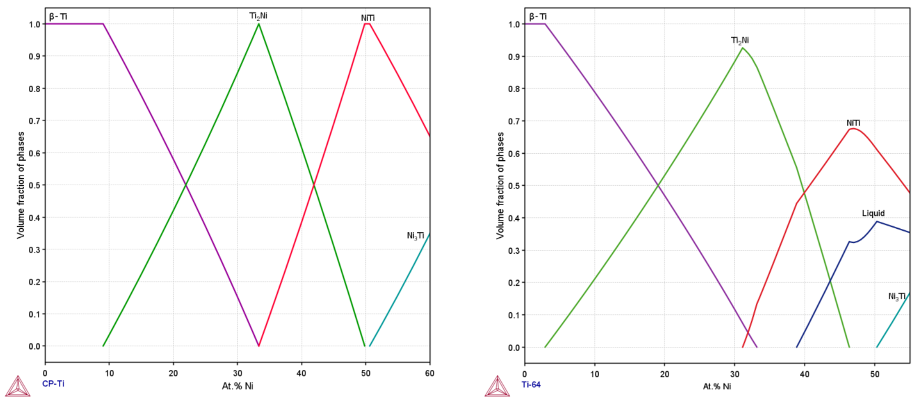

Fig. 5: Equilibrium phase fractions predicted by Thermo-Calc at 900°C for (a) CP-Ti/Ni and (b) Ti-64/Ni systems.

4 Conclusion

In this study, we established that surface alloying of CP-Ti and Ti-64 substrates by the weld deposition of Ni is a successful approach for producing hard coatings on Ti-based materials. We determined the spatial variation of composition, microstructure and hardness in these coatings which revealed the formation of hard Ni-Ti IMCs. Specifically, coatings were found be be almost three-times harder than the bare substrate. Thermodynamic simulations were carried out to understand the similarities and differences in phase formation in the two cases which provided valuable insights into underlying solidification mechanisms. Although our study provided promising results in terms of process development and microstructural characterization for both materials, the adoption and performance of the coatings in service will depend on their wear resistance. Therefore, we have undertaken a systematic ball-on-disc wear study on these materials with and without coating. A detailed analysis of the friction and wear results, and a microscopic study of the wear tracks to reveal the underlying wear mechanisms, are currently underway and will be published later.

References

1. Budinski, Kenneth G. "Tribological properties of titanium alloys." Wear 151.2 (1991): 203-217.
2. Dong, H. "Tribological properties of titanium-based alloys." Surface engineering of light alloys. Woodhead Publishing, 2010. 58-80.
3. Tian YS, Chen CZ, Li ST, Huo QH. Research progress on laser surface modification of titanium alloys. Appl Surf Sci 2005;242:177–84.
4. Weng, Fei, Chuanzhong Chen, and Huijun Yu. "Research status of laser cladding on titanium and its alloys: A review." Materials & Design 58 (2014): 412-425.
5. Zhao H, Zhao C, Xie W, Wu D, Du B, Zhang X, et al. Research Progress of Laser Cladding on the Surface of Titanium and Its Alloys. Materials 2023;16.
6. ZHANG, Shu-quan. "Microstructure and wear resistance of laser clad TiB–TiC/TiNi–Ti2Ni intermetallic coating on titanium alloy." Transactions of Nonferrous Metals Society of China 22.7 (2012): 1667-1673.
7. Bai, L. L., et al. "Effect of the content of B4C on microstructural evolution and wear behaviors of the laser-clad coatings fabricated on Ti6Al4V.' Optics & Laser Technology 76 (2016): 33-45.
8. Li M, Huang J, Zhu YY, Li ZG. Effect of heat input on the microstructure of in-situ synthesized TiN-TiB/Ti based composite coating by laser cladding. Surf Coat Technol 2012;206:4021–6
9. Molian PA, Hualun L. Laser cladding of ti-6al-4v with bn for improved wear performance. Wear 1989;130:337–52
10. Song R, Li J, Shao JZ, Bai LL, Chen JL, Qu CC. Microstructural evolution and wear behaviors of laser cladding Ti 2 Ni/α(Ti) dual-phase coating reinforced by TiB and TiC. Appl Surf Sci 2015;355:298–309.
11. Liu H, Zhang X, Jiang Y, Zhou R. Microstructure and high temperature oxidation resistance of in-situ synthesized TiN/Ti3Al intermetallic composite coatings on Ti6Al4V alloy by laser cladding process. J Alloys Compd 2016;670:268–74.
12. Feng Y, Feng K, Yao C, Li Z, Sun J. Microstructure and properties of in-situ synthesized (Ti_3Al+TiB)/Ti composites by laser cladding. Mater Des 2018;157:258–72.
13. Jianing L, Chuanzhong C, Lei Z. Microstructure characteristics of Ti3Al/TiC ceramic layer deposited by laser cladding. Int J Refract Metals Hard Mater 2011;29:49–53.
14. Liu F, Mao Y, Lin X, Zhou B, Qian T. Microstructure and high temperature oxidation resistance of Ti-Ni gradient coating on TA2 titanium alloy fabricated by laser cladding. Opt Laser Technol 2016;83:140–7.
15. Meng Q, Geng L, Ni D. Laser cladding NiCoCrAlY coating on Ti-6Al-4V. Mater Lett 2005;59:2774–7.
16. Sun RL, Lei YW, Niu W. Laser clad TiC reinforced NiCrBSi composite coatings on Ti-6Al-4V alloy using a CW CO2 laser. Surf Coat Technol 2009;203:1395–9.